

## Original Article

## EFFECT OF METHYL SUBSTITUTION IN FLAVONES ON ITS LOCALIZATION AND INTERACTION WITH DPPC MODEL MEMBRANE: IMPLICATIONS FOR ANTI-PROLIFERATIVE ACTIVITY

RAGINI SINHA<sup>a</sup>, AARTI ANANTRAM<sup>b</sup>, URMILA J. JOSHI<sup>\*b</sup>, SUDHA SRIVASTAVA<sup>a</sup>, GIRJESH GOVIL<sup>a</sup><sup>a</sup>National Facility for High Field NMR, Tata Institute of Fundamental Research, Homi Bhabha Road, Mumbai 400005, India, <sup>b</sup>Principal K M Kundnani College of Pharmacy, Cuffe Parade, Mumbai 400005, India  
Email: urmilajoshi@hotmail.com

Received: 01 Mar 2015, Revised and Accepted: 26 Mar 2015

## ABSTRACT

**Objective:** Flavones are an important class of naturally occurring molecules possessing multiple pharmacological activities. The anti-proliferative activity is associated with the ability of flavones to influence membrane-dependent processes. We have investigated the localization and interaction of the synthesized flavones: 4'-methylflavone (4MF) and 4'-methyl-7-hydroxy flavone (4M7HF) with 1,2-dipalmitoyl-sn-glycero-3-phosphocholine (DPPC) model membrane.

**Methods:** Differential Scanning Calorimetry (DSC) and multi nuclear NMR was used to study the interactions with DPPC model membrane. The extent of interaction of these compounds has been compared with the parent molecules: flavone (FLV) and 7-hydroxy flavone (7HF).

**Results:** Results of DSC and NMR indicate that FLV partitions deepest inside the hydrophobic core and 7HF is localized mostly at the lipid/water interface. 4MF and 4M7HF lying in between the hydrophilic and hydrophobic core. All four molecules assume a mixed orientation with respect to the bilayer normal as indicated by chemical shifts of the lipid protons in NMR. Interaction with the membrane follows the order FLV>4MF>4M7HF>7HF. Radical scavenging activity parallels the presence of hydroxyl groups. Although FLV interacts highest with the membrane, it does not show highest antiproliferative activity. Interaction of the compounds with protons 3, 5a and 7 of DPPC is improved by the methyl substitution on the B-ring, so is the antiproliferative activity.

**Conclusion:** That's antiproliferative activity of the compounds is at least partially related to the interaction of these molecules with the lipid water interface region.

**Keywords:** Flavones, DPPC, Anti-proliferative activity, Anti-oxidant effect, DSC, NMR.

## INTRODUCTION

Flavonoids are a group of polyphenolic compounds, with a diphenylpropane skeleton. These compounds are associated with a broad spectrum of pharmacological activities [1]. Chrysin, (5, 7-dihydroxyflavone) is one of the major naturally occurring flavones. It possesses anti-proliferative, antioxidant and anti-inflammatory activity [2]. Antioxidant activity of the naturally occurring flavones has been extensively studied [3]. It is well documented in the literature that antioxidant properties of flavonoids are dependent upon the number and position of the phenolic hydroxyl groups [4]. Even simple monohydroxy flavones derivatives such as 7-hydroxy flavone possess significant antioxidant effects [5]. The antioxidant activity is partially associated with the ability of the flavone to interact with various regions of the membrane [6].

Several mechanisms have been proposed to explain the anti-proliferative activity of chrysin and its analogs [7-8]. Our previous work on naturally occurring flavonoids indicated that the anti-proliferative activity of the compounds was affected by localization and interaction of those compounds with lipid bilayers [9]. Quercetin with highest anti-proliferative activity was shown to localize and interact with the lipid water interface region whereas unsubstituted flavone (FLV) was localized deeper in the lipid bilayer. To probe further into the relationship between anti-proliferative activity, localization and interactions with the lipid bilayer, we synthesized substituted flavones viz. 4'-methylflavone (4MF) and 4'-methyl-7-hydroxy flavone (4M7HF) and compared their interaction with 7HF and FLV in relation to their antioxidant and anti-proliferative activities.

## MATERIALS AND METHODS

## Materials

Flavone, 7-hydroxyflavone, 1, 2-dipalmitoyl-sn-glycero-3-phosphocholine (DPPC), 2, 2-diphenyl-1-picrylhydrazyl (DPPH), benzoic acid, phosphorous pentachloride (PCl<sub>5</sub>) and 2-

hydroxyacetophenone were purchased from Sigma chemicals Co. USA. The solvents used were of AR grade.

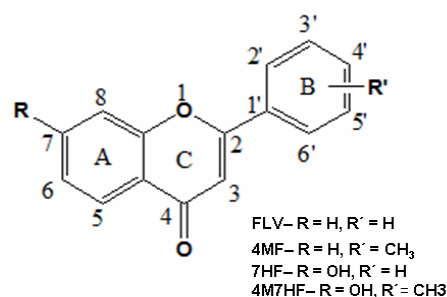
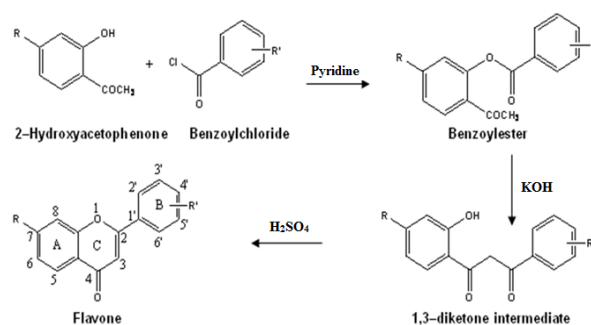


Fig. 1: Structure of Flavone (FLV), 4'-methylflavone (4MF), 7-hydroxyflavone (7HF) and 4'-methyl-7-hydroxyflavone (4M7HF)

## Synthesis

A mixture of 2, 4-dihydroxyacetophenone (6.8 gm, 0.05 mol), benzoyl chloride (14.03 gm, 0.07 mol) or substituted benzoyl chloride and dry pyridine (10 ml) was shaken for 0.5 h. and then was poured onto crushed ice containing HCl (1M, 250 ml). The product was filtered and washed with ice-cold methanol (10 ml) and then with water. The product obtained was placed in dry pyridine and was stirred with powdered potassium hydroxide followed by acidification with 10% acetic acid to give 1, 3-propanedione derivative. It was refluxed with sulphuric acid and then poured on crushed ice to give the desired flavones (Scheme 1) which were recrystallized from methanol and purified by column chromatography over silica gel to obtain pure flavones (fig. 1). The flavones were characterized by elemental analysis and NMR ( $^1\text{H}$ ,  $^{13}\text{C}$  and COSY). The values of  $^1\text{H}$  and  $^{13}\text{C}$  NMR spectral peak positions (in ppm) are given in table 1.

## Determination of drug-MLV binding constants

Drug-MLV binding constants were determined by the centrifugation method [10] with some modification. MLV's was prepared by varying the lipid concentration from 0.25 mg/ml to 2 mg/ml with fixed drug concentration of 100  $\mu\text{M}$ . This corresponds to a drug:lipid ratio in the range 1:2.5 to 1:20. The resulting MLV's were incubated with water for 2 h, vortexed and subsequently transferred

into ultracentrifuge tubes. Separation of liposomes from the aqueous phase was achieved by centrifugation at 40,000 rpm for 2 h. To the water supernatant was added methanol to make a solvent mixture containing only 10% methanol. The drugs were also dissolved in a solvent with the same ratio of water and methanol. Optical density of 100  $\mu\text{M}$  solution of the pure drug was measured at a wavelength range of 220–400  $\lambda$ . The amount of drug bound to liposomes was determined from the difference in optical density measured for the pure drug and that of the unbound drug present in the supernatant. The drug-liposome apparent binding constant (k) has been analyzed using the double reciprocal plot of the fraction bound versus lipid concentration which yields a straight line with a slope  $1/k$ .

## NMR and DSC experiments

NMR spectra were recorded on a BRUKER AVANCE 500 MHz NMR spectrometer. 2D-COSY and 2D-NOESY spectra were recorded using standard pulse programs [11, 12], with a mixing time of 400 ms.  $^{31}\text{P}$  and  $^{13}\text{C}$  NMR experiments were carried out with a relaxation delay of 1s using broadband proton decoupling. NMR software Topspin 2.0 was used for data processing. DSC measurements were performed on differential scanning calorimeter VP-DES (Microcal, Northampton, MA, USA) by a procedure used earlier [13]. Repeated scans for the same samples were generally super impossible. Data was analyzed with the software ORIGIN provided by Microcal.

Table 1:  $^1\text{H}$  and  $^{13}\text{C}$  NMR chemical shifts (ppm) for flavones in DMSO- $d_6$  at 323K

$^1\text{H}$	$^{13}\text{C}$	FLV		4MF		7HF		4M7HF	
		$^1\text{H}$	$^{13}\text{C}$	$^1\text{H}$	$^{13}\text{C}$	$^1\text{H}$	$^{13}\text{C}$	$^1\text{H}$	$^{13}\text{C}$
H3	C2		163.2		163.5		163.4		163.2
	C3	7.01(s)	107.5	7.01(s)	106.9	6.86(s)	107.2	6.86(s)	103.0
	C4		177.6		177.6		176.9		177.1
H5	C5	8.08(d)	125.2	8.06(d)	125.9	7.91(d)	127.0	7.89(d)	127.0
H6	C6	7.52(t)	126.0	7.52(t)	125.3	6.94(m)	115.6	6.93(dd)	115.5
H7	C7	7.85(t)	134.7	7.85(t)	134.7		162.6		162.6
H8	C8	7.78(d)	118.9	7.81(d)	118.9	7.01(d)	103.1	7.01(d)	106.5
	C9		156.2		156.3		158.1		158.0
	C10		123.8		123.9		116.7		116.7
	C1'		131.7		128.9		131.9		129.0
H2'	C2'	8.10(d)	126.8	8.02(d)	126.8	8.04(d)	126.7	7.96(d)	126.6
H3'	C3'	7.61(m)	129.5	7.41(d)	130.2	7.58(m)	129.6	7.39(d)	130.2
H4'	C4'	7.62(m)	132.2		142.6	7.59(m)	132.0		142.2
H5'	C5'	7.61(m)	129.5	7.41(d)	130.2	7.58(m)	129.6	7.39(d)	130.2
H6'	C6'	8.10(d)	126.8	8.02(d)	126.8	8.04(d)	126.7	7.96(d)	126.6
7OH						10.71(s)		10.81(s)	
4'CH <sub>3</sub>	CH <sub>3</sub>			2.42(s)	21.6			2.41(s)	21.6

## Sample preparation

Multilamellar vesicles (MLV's) from DPPC were prepared using standard procedure [14]. The desired quantity of DPPC and drug were dissolved in chloroform. The solvent was evaporated with a stream of nitrogen so as to deposit a lipid film on the walls of the container. The last traces of the solvent were removed under vacuum. MLV's sample thus prepared was hydrated with the required amount of D<sub>2</sub>O at pH 7.2, followed by incubation in the water bath at 50°C with repeated vortexing. The lipid concentration for NMR samples was maintained at 100 mM while the concentrations of the flavones were varied from 10 to 50 mM. For DSC experiments, samples were prepared by mixing the lipid and drug solutions to obtain drug/lipid ratios from 1:20 to 1:2 by maintaining the lipid concentration to 50 mM. Unilamellar vesicles (ULV's) for NMR experiments were prepared by sonicating the lipid dispersions using a Branson Sonicator-450 at 50% duty cycles till optical clarity was obtained.

## Determination of antioxidant activity by DPPH Assay

Varying concentrations of each drug (0–200  $\mu\text{g/ml}$ , 0.5 mL in methanol) were added to methanolic solution of DPPH (0.1 mM, 1.0 mL) and Tris-HCl buffer (0.1 M, pH 5.5, 1.0 mL) to make a total volume 2.5 mL. The absorbance of the sample was measured at 517

nm after 0.5 h of incubation [15]. The reaction solution without DPPH was used as a blank test. Measurements were performed in triplicate. Free radical scavenging activity of the drug was measured as the difference in absorbance between the test sample and the control (sample without drug). Concentration required for a 50% reduction (IC<sub>50</sub> in  $\mu\text{g/ml}$ ) of DPPH radical solution was determined graphically.

## Determination of Anti-proliferative Activity

Anti-proliferative activity was evaluated by the Sulforhodamine B assay method [16]. Three different cell lines, viz. K562, HepG2 and MCF-7 were used. Cell lines were grown in RPMI 1640 medium containing 10% fetal bovine serum and 2 mM of L-glutamine. The test compounds were dissolved in dimethyl sulfoxide and diluted suitably before adding them to the culture medium. After incubation at standard conditions for 48 h, percent growth inhibition of cells has been calculated.

## RESULTS AND DISCUSSION

### Binding Studies

Fig. 2 shows a plot of fraction of drugs bound to MLV's with increasing concentration of lipid. In all cases, an increase in binding affinity is observed with increasing concentration of lipid. 4MF and

FLV show higher binding as compared to 4M7HF and 7HF. Double inverse plot of the fraction of drug bound vs. inverse of lipid concentration (inset fig. 2) has been used to calculate the binding constants. The results indicate that these molecules bind to the MLV's with variable degree of affinity, in the order, FLV>4MF>4M7HF>7HF. The apparent binding constants measured are: FLV: 3125 M<sup>-1</sup>, 4MF: 2304 M<sup>-1</sup>, 4M7HF: 1030 M<sup>-1</sup> and 7HF: 851 M<sup>-1</sup>. It may be noted that introduction of methyl group as in 4M7HF enhances its binding as compared to 7HF. The possible hydrophobic interactions between FLV and the alkyl region of the lipid bilayer may be responsible for higher binding constant of FLV. The binding of the flavones in context of their thermotropic behavior and dynamics of lipids affecting the intermolecular interactions has been addressed below.

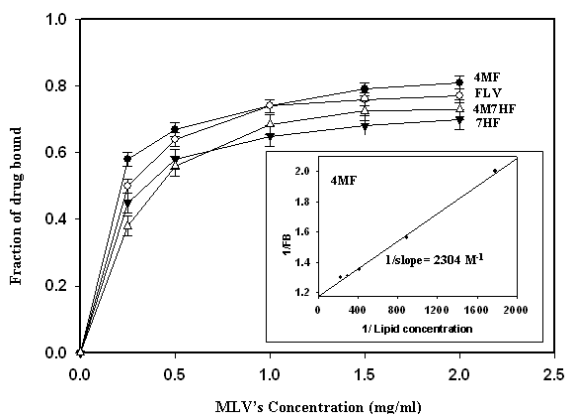


Fig. 2: Binding of FLV (●) 4MF (○) 7HF (▼) and 4M7HF (Δ), with DPPC MLV's

The fraction of drug bound (FB) has been determined by the centrifugation method, as described in the text. The inset fig. shows the double reciprocal plot for 4MF.

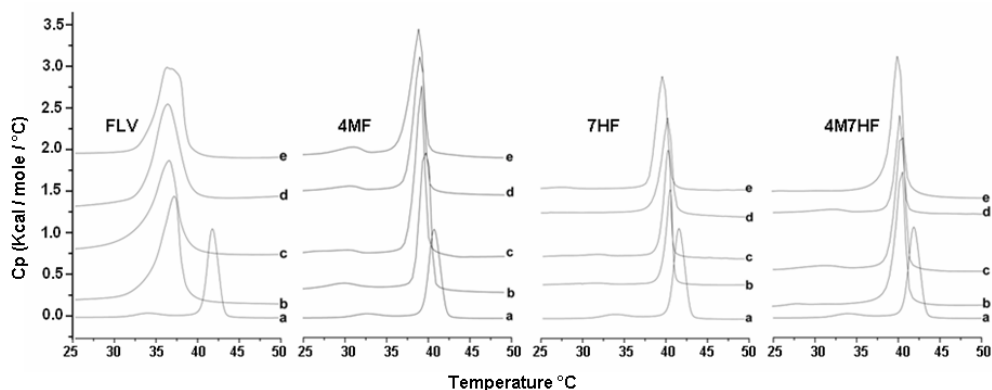


Fig. 3: DSC heating curves of hydrated MLV's of DPPC (50 mM) containing drugs, at drug/lipid molar fractions; a=0.0; b=0.05; c=0.1; d=0.2; e=0.5

Table 2: Pretransition (T<sub>p</sub>) and main transition (T<sub>m</sub>) temperatures of DPPC (50 mM) with varying drug/lipid molar ratios

Drug/DPPC	FLV		4MF		7HF		4M7HF	
	T <sub>p</sub>	T <sub>m</sub>						
Pure	34.10	41.98	34.10	41.98	34.10	41.98	34.10	41.98
DPPC	--	(0.00)	31.26	(0.00)	32.19	(0.00)	27.60	(0.00)
1:20	--	37.16	31.76	40.85	32.05	40.78	31.56	40.53
1:10	--	(4.82)	31.93	(1.13)	27.71	(1.20)	32.54	(1.45)
1:5	--	36.44	32.44	40.42	27.43	40.48	--	40.45
1:2	--	(5.54)		(1.56)		(1.50)		(1.53)
		36.37		40.17		40.34		40.20
		(5.59)		(1.81)		(1.54)		(1.78)
		36.15		39.19		39.86		39.76
		(5.83)		(2.79)		(2.12)		(2.22)

Numbers in brackets indicate difference in the main transition temperature from that of DPPC bilayers.

### DSC studies

DSC is a sensitive technique for studying the effect of drugs on the packing order of lipid bilayers. Thermotropic aspect of drug-lipid interactions can be studied by examining changes in the melting point and the shape of the DSC thermograms [17]. Fig. 3 shows DSC thermograms of DPPC bilayers incorporated with increasing concentrations of FLV, 4MF, 7HF and 4M7HF. In each case, the lower most graphs (a) represent the thermogram for lipid bilayers alone. Here, the pre transition temperature (T<sub>p</sub>) at 34.1 °C indicates the mobility of the choline part of the polar head of DPPC. Mobility of the alkyl chain is reflected in the main transition (T<sub>m</sub>) at 42 °C.

We had reported earlier [9] about the abolition of the pretransition peak of FLV as well as presence of the pretransition peak even at higher concentration of 7HF. The presence of pretransition peak is also seen in the thermograms of 4MF and 4M7HF, indicating the interaction of these molecules with the head group region which stabilizes the membrane architecture [18]. As the molecules penetrate deeper inside the hydrophobic region, the bonding with polar head group region weakens resulting in a concentration-dependent increase in the T<sub>p</sub> values of 4MF and 4M7HF. On the other hand, a decrease in the main transition temperature on addition of the compounds indicates a possible interaction of the molecules with the hydrophobic core of the lipid bilayer. The maximum decrease in T<sub>m</sub> value as observed for FLV (at drug/lipid molar ratio of 1:2) is 5.83 °C as compared to pure DPPC bilayer (table 2). This indicates a strong interaction with the hydrophobic core which enhances the fluidity of the lipid bilayers. Moreover, a broadening of T<sub>m</sub> peak indicates a decrease in co-operativity of the alkyl chain again indicating its localization in the hydrophobic core. The order of decrease in T<sub>m</sub> for the molecules are FLV>4MF>4M7HF>7HF. The hydroxyl groups present on the A-ring of 4M7HF and 7HF probably get involved in hydrogen bonding with part of the head group region and prevent their deeper penetration in the hydrophobic core. This leads to a lesser interaction with the alkyl chain.

### NMR experiments

$^1\text{H}$  and  $^{13}\text{C}$  NMR spectra of FLV, 4MF, 7HF and 4M7HF in  $\text{DMSO-d}_6$  have been assigned using 2D COSY spectrum, literature data and splitting patterns (table 1). Fig. 4 shows an aromatic region of  $^1\text{H}$  NMR spectra of drugs alone (spectra a, b, c and d) and of drugs

incorporated with ULV's of DPPC (spectra a', b', c' and d'). It is observed that in all the four cases, the drug signals arising from aromatic protons become broad on incorporation into lipid bilayers. The chemical shifts are significantly altered and show both downfield and up-field shifts from their original positions.

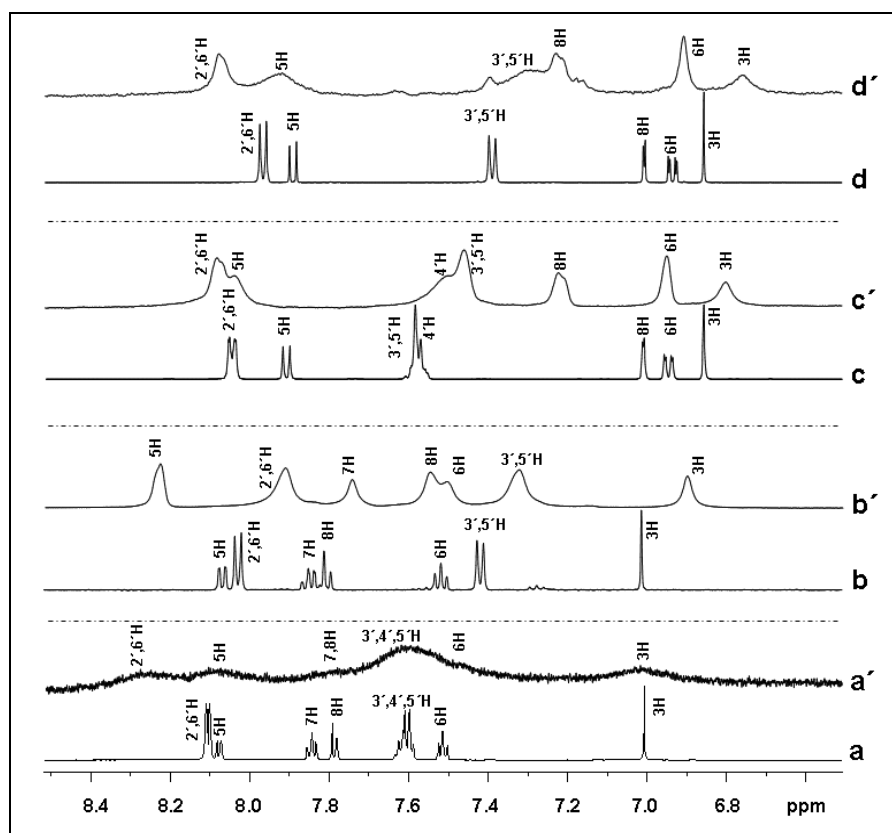


**Fig. 4:** 500.13 MHz  $^1\text{H}$  NMR spectra of aromatic region of pure FLV (a), 4MF (b), 7HF (c) and 4M7HF (d) and that of ULV's of DPPC incorporated with FLV (a'), 4MF (b'), 7HF (c') and 4M7HF (d') in 1:5 drug:lipid molar ratio at 323K in  $\text{D}_2\text{O}$

The protons 3'H and 5'H of 4MF, 7HF and 4M7HF are shifted significantly. This indicates interaction with lipid protons at these positions. On the other hand, in case of FLV the shift of these protons is less but broadening of peak is observed due to interaction. The 8H protons of 7HF and 4M7HF are shifted downfield to a great extent indicating the involvement of 7-OH group in the hydrogen bonding with DPPC. While an up-field shift of 8H proton, in case of 4MF shows its direct interaction with the membrane bilayer. A downfield shift of 5H proton is seen in 4MF, 7HF and 4M7HF but in case of 4MF the downfield shift is highest, again showing its strong interaction. These observations support our results using DSC. It may be pointed out that benzene rings are known to preferentially bind to the hydrophobic core of lipid bilayers. Addition of a hydroxyl group to the ring is likely to shift the location of the ring to the lipid-water interface [19, 20]. In the present study, this is true for 7HF and 4M7HF, where the A-ring containing hydroxyl groups orient towards the lipid-water interface and the B-ring penetrates in the hydrophobic core. In such an orientation, the hydroxyls of the A ring are able to reside at the lipid water interface forming H-bonds, either with water molecules or phosphate and/or acyl oxygens of DPPC. The interaction at the head group region is likely to be a combination of H-bonding and cation- $\pi$  interaction between drug molecule and DPPC. Although FLV does not display the very significant shift of aromatic protons as compared to other compounds, but broadening of peaks indicate a strong interaction of aromatic protons with the membrane.

The comparison of the  $^1\text{H}$  NMR spectra of pure DPPC and ULV's of DPPC incorporated with drugs (1:5 drug/lipid ratios) at 323 K

indicates shift of DPPC protons upon binding with the flavones under study (fig. 5). These shifts can be used for predicting the localization of the compounds in the lipid bilayer. The chemical shifts of the lipid protons also indicates the orientation of the drug molecules with respect to the lipid bilayer normal [21]. The drug molecule imparts ring current effects on the lipid protons, due to which the lipid resonances are known to shift up-field or downfield.

Upon interaction with ring edge the resonances are shifted downfield and on interaction with ring centre it is shifted up-field [22]. Thus, a uniform downfield shift indicates the ring plane to be perpendicular whereas a uniform up-field shift indicates a parallel orientation of the ring plane with reference to the bilayer normal. Absence of a uniform up-field or downfield shift in all cases indicates mixed orientation of the rings.

Upon binding with FLV there is the significantly large shift in the alkyl chain region of lipid. However, for 4MF and 4M7HF the shift is largest with the *sn*-1-glycero group followed by polar head region. The above chemical shift pattern of the lipid protons in the presence of drugs, indicates that FLV interaction is mostly at the hydrophobic core while, that of 4MF, 7HF and 4M7HF interaction is mostly at the lipid/water interface. A perpendicular orientation with respect to the hydrophobic core is seen in case of FLV. 7HF show minimum but uniform interaction at all regions. To probe deeper into the nature of interaction,  $^1\text{H}$ - $^1\text{H}$  NOESY spectra of ULV's of DPPC and of those incorporated with drugs have been recorded (fig. not shown). 2D NOESY spectra of FLV, 4MF, 7HF and 4M7HF incorporated with ULV's show both intramolecular and intermolecular NOEs indicative

of their interaction with lipid bilayer. In the case of FLV, protons H3' and H5' of ring B show NOEs (close proximity) with the  $(\text{CH}_2)_n$  protons. In case of 7HF and 4M7HF, protons of rings A and C show close proximity largely with the head region-N $(\text{CH}_3)_3$  protons. This

indicates that these molecules are largely residing in the polar head region with some penetration in the hydrophobic core. This supports our earlier discussions that only FLV is partitioning deeper into the hydrophobic core.

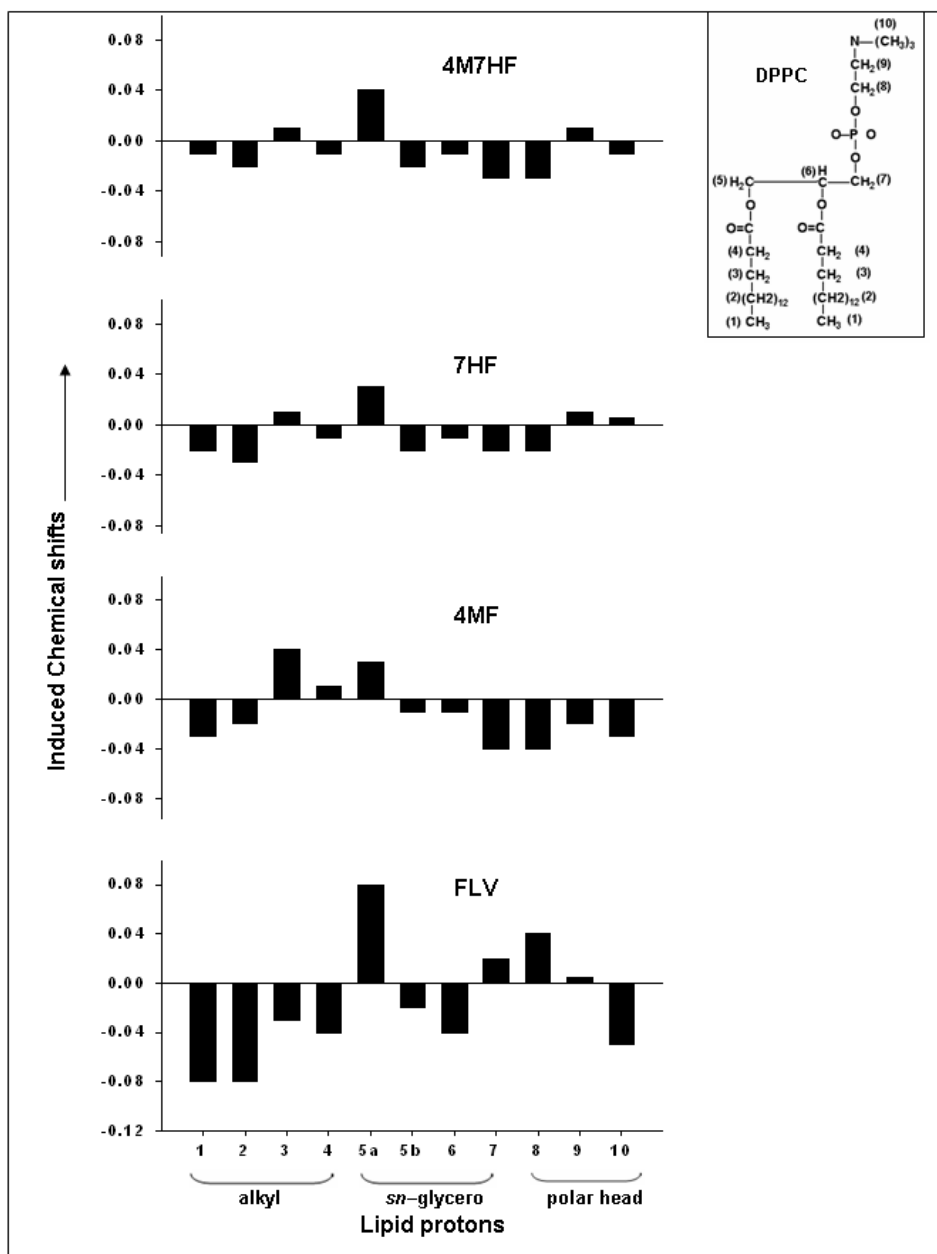


**Fig. 5: Ring current induced chemical shift changes in the signals of ULV's of DPPC incorporated with drugs in 1:5 drug/lipid molar ratio at 323K in the presence of FLV, 4MF, 7HF and 4M7HF. Chemical shifts are either up-field (+) or downfield (-), depending on the orientation of the drug molecule with respect to the bilayer normal**

In the  $^{13}\text{C}$  NMR of the DPPC ULV and that of ULVs incorporated with FLV, 4MF, 7HF and 4M7HF, all the signals arising from drugs are broadened compared to their pure form (fig. 6). The broadening of the signals arises due to an exchange at an intermediate NMR time scale between the bound and free form of these molecules [23]. However, signals arising from lipid mostly remain sharp. A broadening of the peak is observed in the FLV, 4MF and 4M7HF incorporated ULV vesicles in carbon atom 5 belonging to *sn*-1-glycero group of lipid (indicated by \* in the vertical expansion of fig. 6) showing its interaction with the drug molecule. In the case of ULV vesicles incorporated with 7HF this peak remains sharp. This further supports our observation that unlike 7HF which is mostly localized

at the polar head region of lipid/water interface the other molecules are located deeper inside and interact at the *sn*-glycero region.

$[^{31}\text{P}]$  NMR is sensitive to local motions and the orientation of the phosphate group in the membrane. It has been used for monitoring structural changes and detecting polymorphism in model membranes [24]. Effect of FLV, 4MF, 7HF and 4M7HF on  $[^{31}\text{P}]$  line shape has been monitored at varying temperature and concentrations. It may be noted here that these molecules do not alter the characteristic line shapes exhibiting bilayer features of the MLV's of lipid at all concentrations (Supplementary fig. 1). However, FLV molecule, show a change in the  $[^{31}\text{P}]$  line shape from bilayer to

hexagonal phase at 1:2 drug/lipid molar ratio. Lipid bilayers give a characteristic broad spectrum with a high field peak and low field shoulder. Chemical shift anisotropy (CSA) can be measured from the

low and high field shoulders of the spectrum ( $\sigma_{\parallel}$  and  $\sigma_{\perp}$ -components). The CSA of the phosphate group has been used to determine the molecular motions near the bilayer head groups [25].

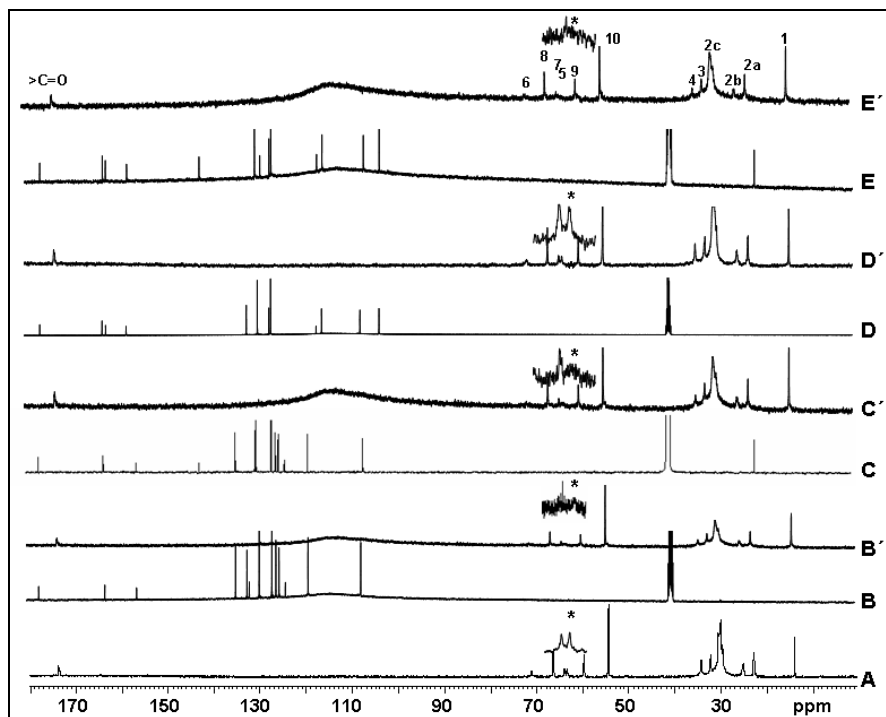


**Fig. 6:** 125.7 MHz  $^{13}\text{C}$  NMR spectra of the ULV's of DPPC (A) and ULV's of DPPC incorporated with FLV (B'), 4MF (C'), 7HF (D') and 4M7HF (E') in 1:5 drug/lipid molar ratio at 323K in  $\text{D}_2\text{O}$ . The  $^{13}\text{C}$  NMR spectrum of pure drug molecules FLV (B), 4MF (C), 7HF (D) and 4M7HF (E) in  $\text{DMSO-d}_6$  is also shown. Peaks for carbon atoms 5 and 7 have been vertically expanded to show up-field shift as indicated by \*

The effect of FLV, 4MF, 7HF and 4M7HF on the [31] PCSA has been measured as a function of concentration and temperature is shown in fig. 7. The amount by which the CSA is reduced is related to the allowed amplitude of the motion [26]. At 323K (phase transition temperature), in case of 7HF, the CSA increases with increasing concentration indicating restricted motion of the head group due to binding. The molecule is likely to form hydrogen bonds with the phosphate oxygens or water molecules which are present in the vicinity, thereby causing a decrease in the local mobility of phosphorus and a consequent increase in CSA. FLV, 4MF and 4M7HF on the other hand impart constant decrease in CSA with increasing concentration indicating a relatively free motion of the head region

of lipid bilayer. This is due to the binding of these molecules to the interior hydrophobic core of the lipid bilayer with the consequent increase in membrane fluidity, as also observed in case of DSC results. Similar trends in change in CSA are observed below and above phase transition (at 303K and 333 K) as well for all four molecules. The highest decrease in CSA is observed in case of 4MF molecule followed by 4M7HF and 7HF. However, in case of FLV phase transformation starts at higher temperature, due this, its CSA starts increasing. Therefore, based on the above NMR results we can say that FLV is partitioning deepest inside the hydrophobic core and 7HF is localized mostly at the lipid/water interface. 4MF and 4M7HF lying in between the hydrophilic and hydrophobic core.

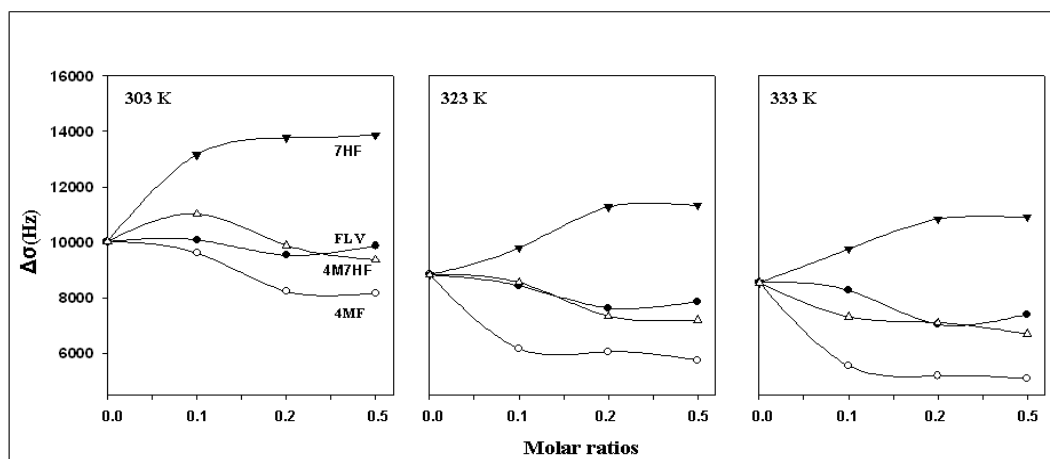


**Fig. 7:** Change in CSA (Hz) of DPPC ULV's on increasing concentration of FLV (●) 4MF (○), 7HF (▼) and 4M7HF (Δ). Temperatures are 303K, 323K and 333K in  $\text{D}_2\text{O}$

### Anti-oxidant and anti-proliferative activity

DPPH assay has been used to estimate the radical scavenging and antioxidant activity of flavonols [27]. The radical scavenging activity is known to depend on the number and the position of the phenolic-OH groups [28]. The molecules 7HF and 4M7HF possess OH group on ring A therefore they show highest antioxidant activity. The antioxidant property of these molecules varies in the order 7HF>4M7HF>>4MF>FLV and depends upon the presence of hydroxyl group. These results are in accordance with the presence of 7-OH group which is responsible for the radical scavenging activity. The anti-proliferative activity of the flavones is shown against K562, HepG2 and MCF-7 cell lines in table 3. In our previous paper [9] on the naturally occurring flavones, we had observed that Baicalein and 6-HF show a significant antiproliferative activity as compared to other naturally occurring flavones. A closer look at the values of induced chemical shifts indicates that these compounds interact significantly with the protons 3, 5a and 7 (numbers according to fig.

5) of DPPC. Same was the case with the synthetic flavones. Our work on 4'-nitroflavone [29] also indicates that interaction of this compound with protons 3, 5a and 7 of DPPC paralleled its considerable antiproliferative activity. Extending these observations to the compounds under the present study, we can observe that none of the present flavones 4MF and 4M7HF interact significantly with all these protons (3, 5a and 7) of DPPC. They also do not possess considerable antiproliferative activity. However, if we compare them to their base moieties their activities seem to be improved. 4MF shows greater effect against K562 and MCF-7 cell lines as compared to FLV. Similarly, 4M7HF shows greater effect against K562 and HepG2 as compared to 7HF. These effects parallel the improved interactions of these compounds with protons 3, 5a and 7 of DPPC. Therefore, we can say that incorporating methyl group at 4'-position of the respective flavones alters the localization and interaction of these compounds in the model lipid membrane, which has direct implications on the antiproliferative activity of these compounds.

**Table 3: *In vitro* antioxidant activity (by DPPH radical scavenging method) and antiproliferative activity (on cell growth of different human cancer cell lines) of flavones**

Flavones	DPPH radical scavenging activity IC <sub>50</sub> (µg/ml) <sup>a</sup>	% Growth of different human cancer cell lines <sup>b</sup>		
		MCF-7	K562	HepG2
FLV	>100	50.2	58.6	-9.6
4MF	52.1	30.2	41.1	71.8
7HF	24.2	26.9	22.3	98.8
4M7HF	25.6	32.0	21.5	82.0

<sup>a</sup>The molar drug concentrations required to cause 50% inhibition (IC<sub>50</sub>) were determined from dose-response curves. <sup>b</sup>Concentration of flavones is 10<sup>-4</sup> µg/ml. Results represent means±SD of at least three different experiments.

### CONCLUSION

The objective of the present study was to establish the effect of substitution at 4'-position of the flavones on their localization, interactions with DPPC and pharmacological activity. It has been shown that localization of these compounds depends upon the nature of the substituents and interaction of these molecules plays an important role in their antiproliferative activity. From the present work, it may be concluded that antiproliferative activity of the compounds is at least partially related to the interaction of these molecules with the lipid water interface region.

### ACKNOWLEDGEMENT

Ragini Sinha and Girjesh Govil thank the Indian National Science Academy and Urmila Joshi thanks University Grants Commission (F. No. 41-745/2012 (SR)) for funding the above project. The help provided by National Facility for High Field NMR located at TIFR are gratefully acknowledged.

### CONFLICT OF INTERESTS

Declared None

### REFERENCES

1. E Middleton, C Kandaswami, TC Theoharides. The effects of plant flavonoids on mammalian cells: Implications for inflammation, heart disease and cancer. *Pharm Rev* 2002;52:103-8.
2. GK Harris, Y Qian, SS Leonard, DC Sbarra, X Shi. Luteolin and chrysin differentially inhibit cyclooxygenase-2 expression and scavenge reactive oxygen species but similarly inhibit prostaglandin-E2 formation in RAW 264.7 cells. *J Nutr* 2006;136:1517-21.
3. V Cody, E Middleton, JB Harborne, A Beretz. *Plant Flavonoids in biology and medicine II*. Biochemical, pharmacological and structure-activity relationships. A. R. Liss: New York; 1987.
4. HA Scheidt, A Pampel, L Nissler, R Gebhardt, D Huster. Investigation of the membrane localization and distribution of flavonoids by high-resolution magic angle spinning NMR Spectroscopy. *Biochem Biophys Acta* 2004;1664:97-107.
5. G Pushpavalli, P Kalaiarasi, C Veeramani, KV Pugalendi. Effect of chrysin on hepatoprotective and antioxidant status in D-galactosamine-induced hepatitis in rats. *Eur J Pharmacol* 2010;631:36-41.
6. PI Oteiza, AG Erlejman, SV Verstraeten, CL Keen, CG Fraga. Flavonoid-membrane interactions: A protective role of flavonoids at the membrane surface? *Clin Dev Immun* 2005;12:19-25.
7. S Chaudhari, B Pahari, PK Sengupta. Ground and excited state proton transfer and antioxidant activity of 7-hydroxyflavone in model membranes: Absorption and fluorescence spectroscopic studies. *Biophys Chem* 2009;139:29-36.
8. T Zhang, X Chen, L Qu, J Wu, R Cui, Y Zhao. Chrysin and its phosphate ester inhibit cell proliferation and induce apoptosis in Hela cells. *Bioorg Med Chem* 2004;12:6097-105.
9. Ragini Sinha, Manoj K Gadhwal, Akshada Joshi, Urmila J Joshi, Sudha Srivastava and Girjesh Govil. Localization and interaction of hydroxy flavones with lipid bilayer model membrane. *Eur J Med Chem* 2014;80:285-94.
10. HY Cheng, CS Randall. Carvedilol-liposome interaction: evidence for strong association with the hydrophobic region of the lipid bilayers. *BBA-Biomembranes* 1996;1284:20-8.
11. WP Aue, E Bartholdi, R Ernst. Two dimensional spectroscopy. Application to nuclear magnetic resonance. *J Chem Phys* 1976;64:2229-46.
12. FAL Anet, AJR Bourn. Nuclear magnetic resonance spectral assignments from nuclear overhauser effects. *J Am Chem Soc* 1965;87:5250-1.
13. R Sinha, MK Gadhwal, UJ Joshi, S Srivastava, G Govil. Interaction of quercetin with DPPC model membrane: Molecular dynamic simulation, DSC and multinuclear NMR studies. *J Indian Chem Soc* 2011;88:1203.
14. RD Kornberg, HM McConnel. Inside-outside transitions of phospholipids in vesicle membranes. *Biochem* 1971;10:1111-20.
15. P Molyneux. The use of the stable free radical diphenylpicrylhydrazyl (DPPH) for estimating antioxidant activity. *J Sci Technol* 2004;2:211-9.
16. V Vichai, K Kirtikara. Sulforhodamine B colorimetric assay for cytotoxicity screening. *Nat Protoc* 2006;1:1112-6.

17. M Polikandritou Lambros, E Sheu, JS Lin, HA Pereira. Interaction of a synthetic peptide based on the neutrophil-derived antimicrobial protein CAP37 with dipalmitoyl-phosphatidylcholine membranes. *BBA-Biomembranes* 1997;1329:285-90.
18. RF Epanand, A Ramamoorthy, RM Epanand. Membrane lipid composition and the interaction of pardaxin: The role of cholesterol. *Prot Pept Lett* 2006;13:1-5.
19. D Bassolino-Klimas, HE Alper, TR Stouch. Mechanism of solute diffusion through lipid bilayer membranes by molecular dynamics simulation. *J Am Chem Soc* 1995;117:4118-29.
20. K Kachel, E Asuncion-Punzalan, E London. Anchoring of tryptophan and tyrosine analogs at the hydrocarbon-polar boundary in model membrane vesicles. *Biochem* 1995;34:15475-9.
21. T Kimura, K Cheng, KC Rice, K Gawrisch. Location, structure, and dynamics of the synthetic cannabinoid ligand CP-55, 940 in lipid bilayers. *Biophys J* 2009;96:4916-24.
22. H Stamm, H Jaeckel H. Relative ring current effects based on a new model for aromatic-solvent-induced shift. *J Am Chem Soc* 1989;111:6544-50.
23. YK Levine, P Partington, GCK Roberts, NMJ Birdstall, JC Metcalfe. <sup>13</sup>C Nuclear Magnetic relaxation times and models for chain molecules in Lecithin vesicles. *FEBS Lett* 1972;23:203-7.
24. S Srivastava, RS Phadke, G Govil. Role of tryptophan in inducing polymorphic phase formation in lipid dispersions. *Indian J Biochem Biophys* 1988;25:283.
25. PR Cullis, MJ Hope, CPS Tilcock. Lipid polymorphism and the role of lipids in membranes. *Chem Phys Lipids* 1986;40:127-44.
26. J Frenzel, K Arnold, P Nuhn. Calorimetric <sup>13</sup>C NMR and <sup>31</sup>P NMR studies on the interaction of some phenothiazine derivatives with dipalmitoyl phosphatidylcholine model membranes. *Biochem Biophys Acta* 1978;507:185-97.
27. W Brand-Williams, ME Cuvelier, C Berset. Use of a free radical method to evaluate antioxidant activity. *Lebensm Wiss Technol* 1995;28:25-30.
28. SABE van Acker, MJ de Groot. A quantum chemical explanation of the antioxidant activity of flavonoids. *Chem Res Toxicol* 1996;9:1305-12.
29. Ragini Sinha, Urmila J Joshi, Sudha Srivastava, Girjesh Govil. Interaction of chrysin and some novel flavones with DPPC model membrane: study based on MD Simulation, DSC And NMR. *Int J Pharm Biosci* 2014;5(1):364-81.